

Chemico-diffusion kinetics of model epoxy–amine resins

Christopher W. Wise, Wayne D. Cook* and Andy A. Goodwin

Cooperative Research Centre for Polymer Blends, Department of Materials Engineering,
 Monash University, Wellington Road, Clayton, Victoria 3168, Australia
 (Received 12 September 1996)

The curing reaction of stoichiometric mixtures of the diglycidyl ether of bisphenol-A with difunctional diamino diphenyl methane and monofunctional aniline was studied using isothermal differential scanning calorimetry over a range of temperatures. High temperature data, beyond the diffusion controlled range, was used to fit the kinetics to an autocatalytic rate equation to determine the chemically-controlled rate constants. In order to model the effect of diffusion on reaction rate, the Couchman–Karasz equation was used to fit the glass transition temperature (T_g) of partially cured samples to the degree of conversion. This T_g /conversion relationship was used in the Williams–Landel–Ferry (WLF) equation to calculate the diffusional rate constant during cure. The chemical and diffusional rate constants were combined in the Rabinowitch equation to model the overall rate constant for the reaction. This model predicts rate/conversion data and has reasonable agreement with the experimental curves. Differences between theory and experiment were discussed in terms of the dependence of the diffusion coefficient on molecular size and the non-universality of the WLF constants. © 1997 Elsevier Science Ltd.

(Keywords: epoxy resins; chemico-diffusion kinetics; glass transition temperature)

INTRODUCTION

Epoxy resins are thermosetting polymers commonly used as adhesives and as composite materials for structural components. Due to the brittle nature of many tightly crosslinked epoxies, some form of toughening is desirable, while maintaining rigidity and high glass transition temperature (T_g). A common approach¹ has been to dissolve a low molecular weight liquid rubber in the liquid epoxy resin. During cure the rubber precipitates because the accompanying increase in molecular weight of the epoxy raises the free energy of mixing, resulting in a fine dispersion of rubber particles in the epoxy matrix. Thus precipitation is controlled by both the curing kinetics (faster cure causes earlier precipitation), and the miscibility of the rubber (higher miscibility reduces precipitation), both of which depend on the cure temperature, but with opposite dependencies. In order to understand the process of rubber precipitation, these two factors must be studied. Thus, in this study the polymerization kinetics of an amine-cured epoxy resin is studied, to provide a better understanding of the rubber toughening process.

The mechanism of the epoxide–amine reaction process is shown in *Figure 1*. At the beginning of the polymerization process, small linear or branched molecules form, and this process is characterized by a gradual increase in molecular weight². As the reaction proceeds, chain branching becomes more extensive until the gel point is reached where an infinite three-dimensional network is formed and the weight-average

molecular weight becomes infinite². Further polymerization causes additional reactions in the sol and gel fractions, leading to a more highly crosslinked structure².

The cure of an epoxy resin is controlled by the temperature dependence of both the rate of diffusion and the rate of molecular collisions which lead to the formation of the network. As cure proceeds, the increasing size and complexity of the epoxy oligomers restrict diffusion, as does the three-dimensional connectivity that forms in the later stages of cure. In addition, the curing process causes a reduction in the free volume and an increase in T_g , and so an additional decrease in the diffusion rate occurs. When the material is cured at a temperature much greater than the T_g of the fully cured polymer, diffusion may not affect the overall rate of reaction. However in many cases, epoxies are cured at lower temperatures, where diffusion can influence the overall reaction rate and may even determine the degree of cure that is achieved, because once the material has vitrified, the reaction will effectively cease^{3,4}. Thus the study of the effect of diffusion on the reaction of epoxies is necessary to predict the properties of the cured polymer.

Autocatalytic reaction kinetics

The epoxide group can react with primary and secondary amines, as shown in *Figure 1*. These reactions are catalysed^{4,5} by a species which hydrogen bonds to the epoxy group, thereby weakening the C–O bonds and facilitating ring opening. The source of the hydrogen-bonding species is considered^{4,5} to arise from two distinct origins. The first source can be any

* To whom correspondence should be addressed

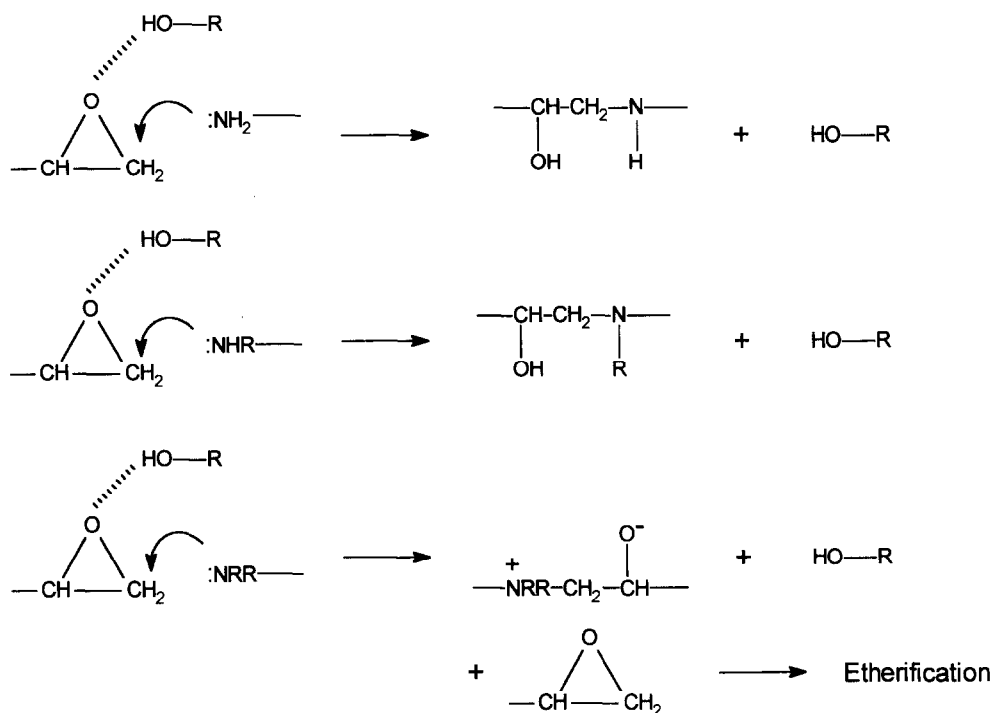
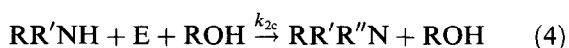
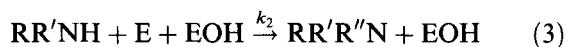
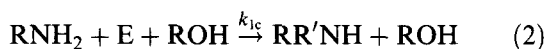


Figure 1 Reaction of epoxide with primary, secondary and tertiary amine

catalytic hydrogen-donating impurity present in the epoxy (e.g. hydroxyl groups in epoxy adducts) while the second catalyst source can be hydrogen bonding species formed (e.g. hydroxyl) or depleted (e.g. amine) during the reaction. Thus the reaction of an epoxy with primary and secondary amines via autocatalysis and impurity catalysis may be expressed as:



where RNH_2 , $\text{RR}'\text{NH}$ and $\text{RR}'\text{R}''\text{N}$ represent the primary, secondary and tertiary amines, E is the epoxy group and EOH and ROH are, respectively, the catalytic hydrogen bonding species which are generated (or depleted) in the reaction or are present in impurities. The rate constants k_1 (equation (1)) and k_2 (equation (3)) refer to the autocatalysed reaction of epoxy with primary and secondary amine respectively, whereas the rate constants k_{1c} (equation (2)) and k_{2c} (equation (4)) relate to the impurity-catalysed reaction of an epoxy with primary and secondary amines, respectively.

The concentration of the adventitious impurity catalyst is assumed to remain constant during the reaction while the concentration of the autocatalytic hydroxyl and amino-hydrogen groups will vary in direct proportion to the amount of epoxy that has reacted. In the analysis first published by Smith⁵ and later by Horie *et al.*⁴, the etherification reaction (Figure 1) is assumed to be insignificant, and catalysis is either by impurities or by hydroxyl groups generated during the reaction. Thus the

rate of consumption of epoxy time t is given by:

$$-\frac{dE}{dt} = k_1EA_1[\text{OH}] + k_2EA_2[\text{OH}] + k_{1c}EA_1C_0 + k_{2c}EA_2C_0 \quad (5)$$

where E is the concentration of epoxide groups, A_1 and A_2 are the concentrations of primary and secondary amines respectively, C_0 is the constant concentration of impurities that catalyse the epoxy amine reaction, and $[\text{OH}]$ is the concentration of hydroxyl groups formed in the reaction. In equation (5) the first two terms on the right hand side represent autocatalysis and the second two terms represent impurity catalysis.

Diffusion models

As noted above, when the T_g of the reacting network approaches the curing temperature, diffusional effects begin to play a role in the kinetics^{3,4}. Chern and Poehlein⁶ used an empirical expression based on the reduction of free volume during cure to model the effect of diffusion control on the polymerization kinetics. Their equation for the overall rate constant multiplies the chemically controlled Arrhenius reaction rate constant (k_{chem}) by a term similar in form to the Williams-Landel-Ferry (WLF) equation:

$$k = k_{\text{chem}} \exp \left[-V^* \left(\frac{1}{V_f} - \frac{1}{V_{fc}} \right) \right] \quad (6)$$

where V_f is the fractional free volume at a given conversion and V_{fc} is the fractional free volume at the gel point, and V^* is a constant with the dimensions of volume. Assuming a linear relationship between conversion and $1/V_f$, Chern and Poehlein⁶ derived the rate constant expression:

$$k = k_{\text{chem}} \exp[-C(\alpha - \alpha_c)] \quad (7)$$

where α_c is the conversion at the gel point and C is a

constant that depends on the structure, system and curing temperature. A similar empirical approach has been used more recently by Kim and Kim⁷, and by Stutz et al.⁸.

Many other authors^{9–12} have taken a more fundamental approach by considering the overall reaction rate to be composed of two components, one associated with the diffusional reaction step and one for the chemical reaction step. When the rate of diffusion is relatively high, the curing kinetics are assumed to be chemically controlled, but when the molecular mobility is constrained, the overall rate of reaction will depend on diffusional effects. Since the time for a reaction step is given by the time for diffusion (inversely related to k_{diff} , the diffusion rate constant) and the time for reaction (inversely related to k_{chem} , the chemical rate constant) the overall rate of reaction, k , is expressed in the Rabino-witch equation⁹:

$$\frac{1}{k} = \frac{1}{k_{\text{diff}}} + \frac{1}{k_{\text{chem}}} \quad (8)$$

where k_{chem} , the chemical rate constant, is given by the Arrhenius equation:

$$k_{\text{chem}} = A_0 \exp\left[\frac{-\Delta E}{RT}\right] \quad (9)$$

Huguenin and Klein¹⁰, and more recently Deng and Martin¹¹, use a WLF-type diffusion equation of the form:

$$k_{\text{diff}} = k_{D_0} D_0 \exp\left[B\left(1 - \frac{1}{f_g + \alpha_f(T - T_g)}\right)\right] \quad (10)$$

where f_g is the fractional free volume at T_g , α_f is the thermal expansion coefficient of the free volume, D_0 is the self diffusion coefficient and k_{D_0} is a constant related to the bonding conditions.

In studies by Wisanrakkit and Gillham³ the diffusional rate constant was given by a WLF-type equation where the denominator is modified by the use of the modulus operator on the term $(T - T_g)$:

$$k_{\text{diff}} = k_{\text{diff}(T_g)} \exp\left[\frac{C_1(T - T_g)}{C_2 + |T - T_g|}\right] \quad (11)$$

Havlicek and Dusek¹² used a similar line of reasoning to those above, but expressed the diffusional rate constant in terms of the Adam–Gibbs theory of cooperative rearrangements:

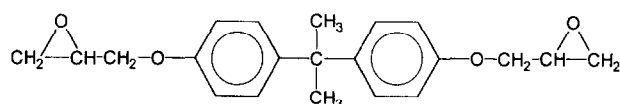
$$k_{\text{diff}} = k_{D_0} D_0 \exp\frac{m}{T \ln[T/(T_g - 50)]} \quad (12)$$

The parameter m (which depends on the discontinuity in heat capacity at T_g and on the configurational entropy and activation energy for a change of configuration) is considered to be a material constant for their analysis¹². Equations (10) and (12) predict a similar temperature dependence for the diffusion rate constant.

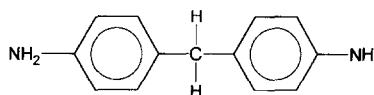
In our study k_{diff} , the diffusional rate constant, is obtained from Smoluchowski¹³:

$$k_{\text{diff}} = 4\pi N_{\text{Av}} r D \quad (13)$$

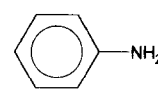
where N_{Av} , r and D are the Avogadro number, the collision radius (which defines the region of space in which the collision process occurs) and the diffusion



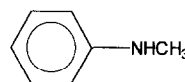
Diglycidyl ether of bisphenol-A



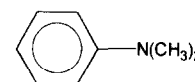
Diamino diphenyl methane



Aniline



N-methyl aniline



Dimethyl aniline

Figure 2 Chemical structures of materials used in this study

constant. If the temperature dependence of the diffusional rate constant is given by the equation¹⁴:

$$\ln\left(\frac{D}{D_{T_g}}\right) = \frac{C_1(T - T_g)}{C_2 + T - T_g} \quad (14)$$

where T_g is the glass transition temperature D_{T_g} is the diffusion constant at T_g , and C_1 and C_2 are constants, then from equations (13) and (14) we have:

$$k_{\text{diff}} = k_{\text{diff}(T_g)} \exp\left[\frac{C_1(T - T_g)}{C_2 + T - T_g}\right] \quad (15)$$

where $k_{\text{diff}(T_g)}$ is the diffusion rate constant at T_g . Since the reactive species, epoxide and amine groups, are in close proximity to one another throughout the reaction, we consider that k_{diff} refers to the segmental diffusion required to bring species within a collision radius. Thus k_{diff} is assumed to be independent of the size of the molecule to which the reactive group is attached. In this paper, the chemico-diffusion model combines equations (8), (9) and (15) to predict the rate constants as a function of temperature.

EXPERIMENTAL

Materials

The epoxy monomer used was the diglycidyl ether of bisphenol-A (DGEBA, Epikote 828, supplied by Shell Chemicals, Australia). The DGEBA was titrated using the HBr technique¹⁵, and the average molecular weight was found to be 372 g mol^{-1} , which compares with 340 g mol^{-1} for pure DGEBA as shown in Figure 2. Four related amines were used as curing agents. Diamino diphenyl methane (DDM) (Ciba-Geigy) is a solid, difunctional aromatic amine with a molecular weight of 198 g mol^{-1} . Aniline (Mallinckrodt Chemical Works) is a liquid monofunctional aromatic primary amine with a molecular weight of 93 g mol^{-1} . N-methyl aniline (NMA, Ajax) is a liquid secondary amine with a molecular weight of 107 g mol^{-1} . Dimethyl aniline is a liquid tertiary amine with a molecular weight of 121 g mol^{-1} . All amines were dried over 4 \AA molecular sieves before use.

Kinetic studies

The reaction of DGEBA with the amines results in a fully crosslinked structure (with DDM) or a linear structure (with aniline), thus yielding polymers of totally different molecular architecture but very similar chemical composition. To investigate the relative reactivity of primary and secondary amines, the monofunctional analogue of aniline, *N*-methyl aniline was also studied.

DDM/DGEBA samples with a stoichiometric ratio of epoxide and amino-hydrogen groups were prepared by melting DDM at around 90°C and mixing with DGEBA heated to the same temperature. The resultant mixture was thoroughly stirred and then cooled rapidly to room temperature, to minimize any cure reaction during preparation. For aniline/DGEBA and NMA/DGEBA mixtures, the amine was dissolved in DGEBA at room temperature to produce a similar stoichiometric mixture. DMA/DGEBA mixtures were prepared at an equimolar ratio.

Fourier transform infra-red spectroscopy (FTi.r., Perkin Elmer 1700) was used to study the extent of final cure by monitoring the epoxy ring resonance¹⁶ at 915 cm⁻¹. For DDM/DGEBA and aniline/DGEBA postcured at 170°C, the conversion was estimated as approximately 90%. It is generally recognized^{17,18} that the mid-infra-red (m.i.r.) technique gives an underestimate of conversion—studies of DGEBA/DDM using near-infra-red (n.i.r.) show that the material can be cured to greater than 95% conversion¹⁸. In this work it is assumed that postcuring above the ultimate T_g provides 100% cure.

A differential scanning calorimeter (d.s.c., Perkin Elmer DSC-7) was used to monitor the cure kinetics. The d.s.c. enthalpy was calibrated using a high purity indium sample; a high purity zinc sample was also used to calibrate the temperature scale. Initial kinetic studies were performed in the scanning mode with the epoxy/amine mixtures being scanned from room temperature to 200°C at a rate of 5°C min⁻¹. Samples of approximately 10 mg were used in sealed pans for all experiments to prevent evaporation of the amines. Measurements of the aniline/DGEBA mixture at the highest curing temperature revealed no measurable mass loss.

The majority of the kinetic studies were performed by isothermal d.s.c. The epoxy amine mixtures were cured at temperatures ranging from 60 to 180°C. The conversions (α) of the epoxy, at cure time t , was determined from the heat evolved up to that time (ΔH), by the expression:

$$\alpha = \frac{\Delta H}{\Delta H_{\max}} \quad (16)$$

where the enthalpy for complete conversion (ΔH_{\max}) was obtained from a plot of the maximum enthalpy vs curing temperature, by taking the asymptote at high temperatures. ΔH_{\max} was found to be 98.9 J mol⁻¹ (420 J g⁻¹) for DDM/DGEBA and 99.1 J mol⁻¹ (426 J g⁻¹) for aniline/DGEBA. This compares with 91.4 J mol⁻¹ found by Barton¹⁹ for the DDM/DGEBA system and values ranging from 100–118 J mol⁻¹ for phenyl glycidyl ether type epoxy/amine reactions tabulated in a review by Rozenberg²⁰. Since the rate is proportional to the rate of heat flow, the rate of conversion is given by:

$$\frac{d\alpha}{dt} = \frac{d(\Delta H)}{dt} \cdot \frac{1}{\Delta H_{\max}} \quad (17)$$

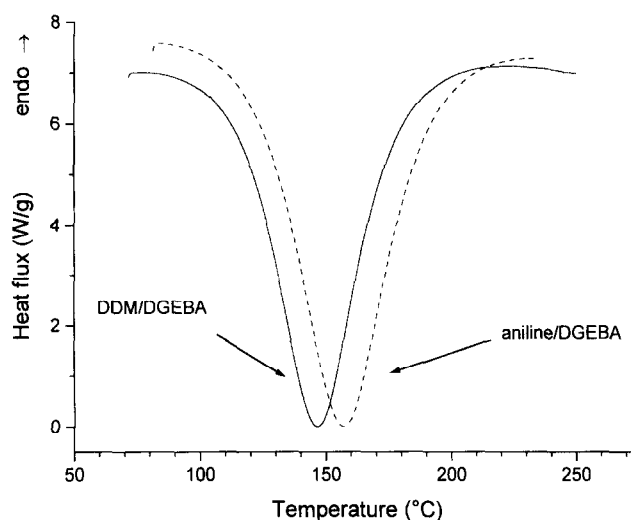


Figure 3 D.s.c. traces for the DDM/DGEBA and aniline/DGEBA systems, 10 mg samples heated at 5°C min⁻¹

Curves of conversion rate vs conversion and conversion vs time were obtained from the isothermal d.s.c. data by numerically integrating the heat flow vs time curves and scaling by ΔH_{\max} .

The d.s.c. was also used to measure the T_g as a function of the degree of cure and cure temperature. The T_g was taken as the midpoint of the transition as determined by the Perkin-Elmer software. T_g -conversion data were obtained by scanning samples in the d.s.c. from -40°C to various temperatures, so that the material was partially cured. The extent of cure was determined by integration of the partial exotherm from the start of the scan up to its termination. The sample was rapidly cooled and re-scanned at 5°C min⁻¹ to give the T_g of the partially cured sample. In undercured samples, an additional exotherm occurred after this glass transition. Summation of the polymerization enthalpies of the first and second exotherms were approximately constant as expected. The T_g was measured as a function of curing temperature by isothermally curing the material beyond the time when the change in heat flux was no longer measurable, indicating that the reaction had ceased. Isothermal curing times ranged from 30 min at 180°C for both the DDM/DGEBA and aniline/DGEBA systems to 5 h at 70°C for the DDM/DGEBA system and 8 h at 70°C for the aniline/DGEBA system. The sample was then cooled and re-heated in scanning mode, at 5°C min⁻¹, to determine the T_g .

RESULTS AND DISCUSSION

Reaction kinetics

The d.s.c. traces in scanning mode for the aniline/DGEBA and DDM/DGEBA mixtures are shown in Figure 3. The DDM/DGEBA mixture reacts at a higher rate than the aniline/DGEBA mixture, even though the monomers have a similar chemical structure. The difference is due to an induction effect, attributable to ring substitution. Based on the observed increase in basicity constants with *para*-substitution of alkyl groups on aniline²¹, the additional aminobenzyl group in the DDM molecule increase the electro-negativity on the nitrogen, making the amine more reactive. This difference in reactivity has also been noted by Charlesworth²²,

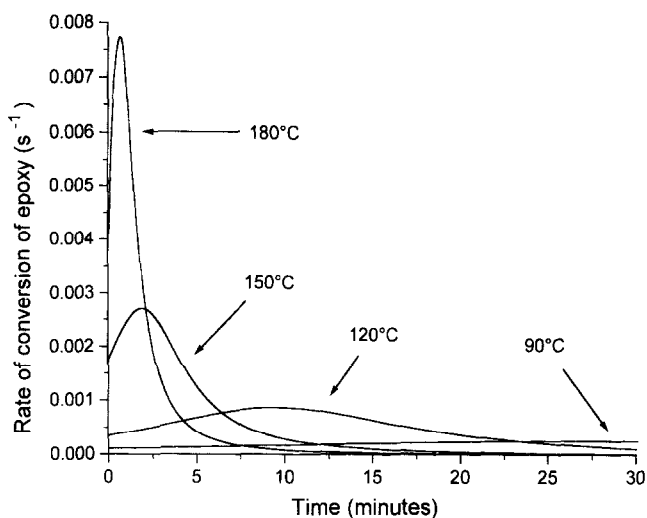


Figure 4 Rate vs time for DDM/DGEBA at various curing temperatures

who found that DDM/DGEBA reacted about $2.5\times$ as fast as the aniline/DGEBA system.

Figure 4 shows representative rate vs time curves obtained by isothermal d.s.c. for the DDM/DGEBA system at different temperatures. At high temperatures, the reaction proceeds rapidly and the rate appears to be chemically controlled. At 90°C the reaction rate is very slow, and does not proceed to 100% conversion due to the very slow rate of diffusion of the reacting species.

The conversion of epoxy (α) is equal to the instantaneous concentration of epoxy groups divided by the initial concentration of epoxy, E_0 . The concentration of hydroxyl groups formed in the reaction is proportional to the conversion and the initial concentration of epoxy and is given by αE_0 . The concentration of epoxide decreases as the reaction proceeds and is therefore equal to $E_0(1 - \alpha)$. Making the assumption⁴ that the reactivity ratio of primary and secondary amine groups is the same for both the self catalysed reaction and the impurity catalysed reaction ($k_2/k_1 = k_{2c}/k_{1c}$) enables the following simplification of equation (5):

$$-\frac{dE}{dt} = k_1 E_0 (1 - \alpha) \left(E_0 \alpha + \frac{k_{1c}}{k_1} C_0 \right) \left(A_1 + \frac{k_2}{k_1} A_2 \right) \quad (18)$$

A further assumption of equal reactivity of primary and secondary amino-hydrogen with epoxy groups means that $k_2/k_1 = 0.5$ if there is no substitution effect. It should be noted that other authors²³ have used an alternative definition of the reactivity ratio where equal reactivity yields a reactivity ratio of unity. If a stoichiometric ratio of epoxy to amino-hydrogen groups is used, then we can equate the number of epoxide groups of the number of amino-hydrogen groups at any conversion:

$$A_1 + \frac{1}{2} A_2 = A_0 - \frac{1}{2} \alpha E_0 = E_0 (1 - \alpha) \quad (19)$$

where A_0 is the initial concentration of primary groups. Since dE/dt is equal to $E_0 \cdot d\alpha/dt$, the rate equation can be further simplified to:

$$\frac{d\alpha}{dt} = k_1 \frac{E_0^2}{2} (1 - \alpha)^2 \left(\alpha + \frac{k_{1c}}{k_1} \frac{C_0}{E_0} \right) \quad (20)$$

which can be re-expressed in terms of two reduced

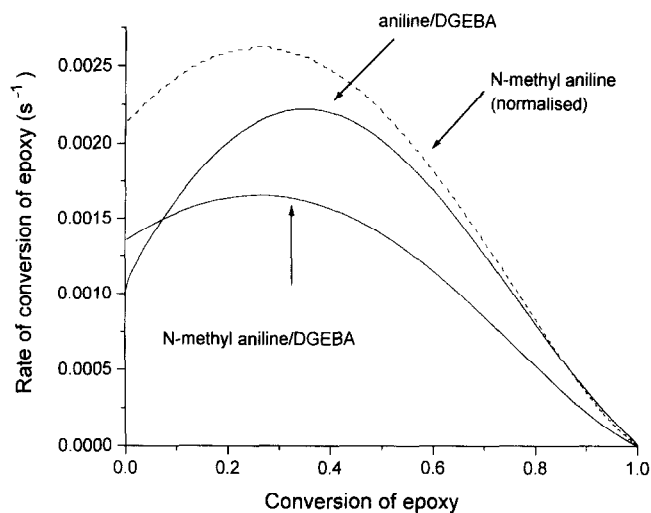


Figure 5 Comparison of reaction rate ($d\alpha/dt$) for aniline and *N*-methyl aniline reacting with DGEBA at 160°C . The normalised curve was obtained by scaling the NMA/DGEBA data to an equivalent concentration of reactive groups as in the aniline/DGEBA system

reaction rate constants:

$$\frac{d\alpha}{dt} = K_1 (1 - \alpha)^2 \left(\alpha + \frac{K_{1c}}{K_1} \right) \quad (21)$$

where $K_1 = k_1 (E_0^2/2)$ and $K_{1c} = k_{1c} (E_0/2) C_0$

Other models^{24,25} assume that the reaction is initially catalysed by amine, but with the simplifications used above the final equation has a similar form. Horie *et al.*⁴ studied the model non-polymerizing epoxy/amine system formed from phenyl glycidyl ether (PGE) and butylamine. Using varying amounts of *n*-butyl alcohol as a hydrogen donating impurity component in order to determine k_{1c} and k_{2c} (as defined in equations (2) and (4)), they showed that the reactivity ratio for the impurity catalysed reaction was close to that of the self catalysed reaction (i.e. $k_{2c}/k_{1c} = k_2/k_1$) and that the measured reactivity ratios (k_2/k_1) were in the range 0.60–0.65. A review by Rozenberg²⁰ tabulates k_2/k_1 ratios measured for a number of amine/epoxy systems, and shows that deviations from equal reactivity occur in both directions but that a negative substitution effect was more commonly observed. Studies by Charlesworth²² suggest that there is no substitution effect associated with primary and secondary amines in the DDM/DGEBA and aniline/DGEBA systems.

The relative reactivity of aniline and *N*-methyl aniline was studied in an attempt to compare primary and secondary amine reaction rates. Figure 5 shows the rate vs conversion curve at 160°C for a NMA/DGEBA mixture with a stoichiometric ratio of amino-hydrogen to epoxy groups. Also shown in this figure is the data for aniline/DGEBA at 160°C . The NMA/DGEBA data is also shown scaled to an equivalent concentration of reactive groups in order for the reaction rates to be directly comparable to the aniline/DGEBA data. At zero conversion the aniline/DGEBA mixture contains only primary amine and the rate is lower than the reaction rate of the secondary amine NMA with epoxy. This implies that the secondary amino-hydrogen groups are more reactive than the primary groups. At high conversions, most of the aniline will be reacted and exist in the form of a secondary or tertiary amine adduct, so the dominant reaction will be between the secondary

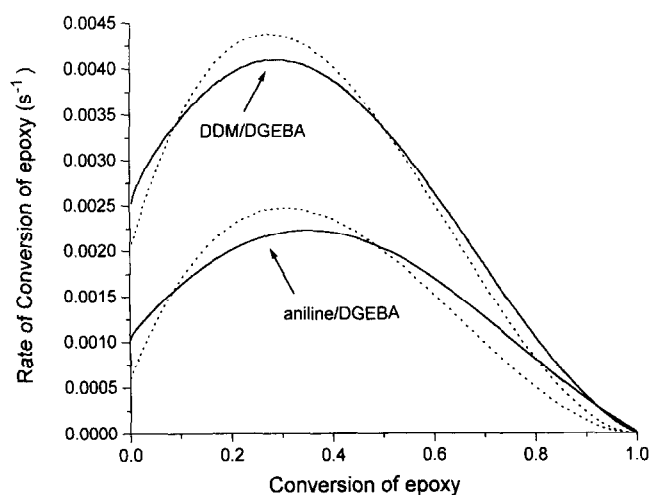


Figure 6 Rate ($d\alpha/dt$) vs conversion at 160°C, for DDM or aniline with DGEBA. The dashed lines are a fit of the DDM/DGEBA and aniline/DGEBA data to equation (21) using the parameters: $K_1 = 0.0229 \text{ s}^{-1}$, $K_{1c} = 0.00202 \text{ s}^{-1}$ for DDM/DGEBA and $K_1 = 0.01478 \text{ s}^{-1}$, $K_{1c} = 0.00060 \text{ s}^{-1}$ for aniline/DGEBA

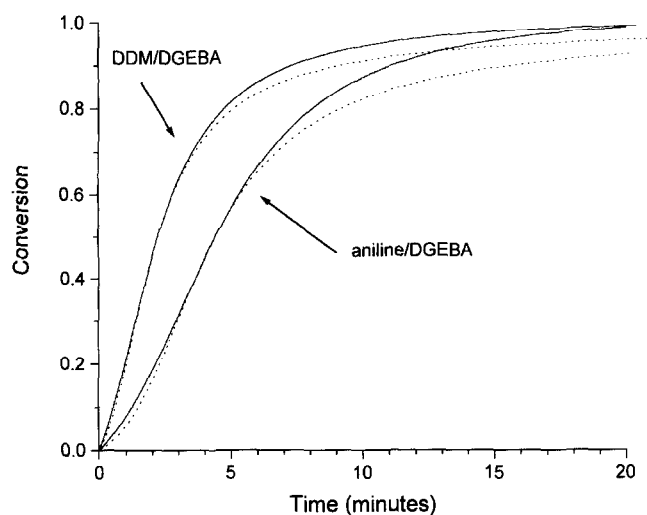


Figure 7 Conversion vs time at 160°C for DDM or aniline with DGEBA. The dashed lines fitted to the DDM/DGEBA and aniline/DGEBA data were calculated with $K_1 = 0.0299 \text{ s}^{-1}$, $K_{1c} = 0.00202 \text{ s}^{-1}$ and $K_1 = 0.01478 \text{ s}^{-1}$, $K_{1c} = 0.00060 \text{ s}^{-1}$ (see Figure 6)

amine and the epoxy. It can be seen that in this case the reaction rates of the aniline/DGEBA and the *N*-methyl aniline/DGEBA system are closer. However we have already noted an induction effect in the comparison of the reactivity of DDM and aniline with epoxy and would expect a difference in the reactivity of *N*-methyl aniline compared with the epoxy/aniline adduct due to the difference in polarity between the methyl group and the hydroxy propyl group. Thus based on this data, a definitive statement about the magnitude of k_2/k_1 is not possible.

Numerical integration of isothermal d.s.c. curves for DDM/DGEBA and aniline/DGEBA yields rate vs conversion and conversion vs time curves such as those shown in Figures 6 and 7. The autocatalytic rate expression (equation (21)) was used to produce a fit to the experimental DDM/DGEBA rate curve obtained at 160°C, and the predicted data are shown in Figures 6 and 7. The agreement between the fit and the experimental curve is not perfect, showing deviation at all conversions. This suggests that equation (21) does not completely

describe the epoxy/amine reaction even at elevated temperatures where the reaction is not affected by diffusion. The similarity of the DDM/DGEBA data to the aniline/DGEBA data suggests that the overall chemical reaction process occurring in the two systems is similar, even though the rate is different.

One possible reason for the imperfect fit of the high temperature experimental data to the auto-catalytic rate equation (Figures 6 and 7) is that the equal reactivity assumption for primary and secondary amine ($k_2/k_1 = 0.5$) is invalid. The d.s.c. technique cannot distinguish between these two reactions, measuring only the overall heat evolved from the reactions. Figure 8 shows the calculated normalized reaction rates (using equation (21)) when k_2/k_1 is varied from 0.125 to 2 but at a constant value of K_{1c}/K_1 . In these graphs there is only a small change in the predicted shape of the curve with large variations in the reactivity ratio, and neither positive nor negative substitution effects would lead to a significantly improved agreement with experimental data.

Another possible reason for the noted discrepancy between the fitted (see equation (21)) curve and experimental results in Figures 6 and 7 is that the kinetic analysis neglects the etherification reaction. Since this reaction is catalysed by tertiary amine such as that produced in the epoxy/amine reaction, dimethyl aniline was used as a tertiary amine analogue of aniline to study the etherification reaction in DGEBA alone. The curing reaction proceeded at a measurable but much lower rate (< 3%) than the DDM or aniline systems. However due to the excessive mass loss (caused by evaporation of the DMA) the data in the present study were not quantitatively analysed. Simon and Gillham²⁶ found the reaction rate constant for the etherification reaction (k_3) to be three orders of magnitude lower than for the primary amine-epoxide reaction (k_1).

Diffusional effects

Figure 9 illustrates the dependence of rate on conversion over a range of temperatures for the DDM/DGEBA system. As expected, as the cure temperature is raised, the rate of polymerization at each level of conversion is markedly increased. At temperatures exceeding 130°C, the level of conversion of epoxy groups was approximately constant. However, at cure temperatures lower than 130°C, the T_g approaches the curing temperature and the segmental mobility within the polymer decreases, thus reducing the rate of diffusion of monomers to reactive sites which in turn reduces the reaction rate. Thus the reaction does not go to complete conversion within the time scale of the experiment. A similar trend is shown for the aniline/DGEBA system (Figure 10), although the effect of diffusion control is not as marked due to the greater molecular mobility allowed by the absence of the crosslinking effect and the lower T_g in the aniline/DGEBA system.

In order to apply the chemico-diffusion model (equations (8), (9), (15) and (21)) to the reaction rate data, it is necessary to determine the T_g as a function of conversion. Figure 11 shows T_g vs conversion for the two systems; the uncured aniline/DGEBA system has a lower initial T_g because the low molecular weight aniline acts as a plasticizer. The T_g at full cure was 165°C for DDM/DGEBA and 85°C for aniline/DGEBA, the difference being due to the effect of crosslinking on T_g for the

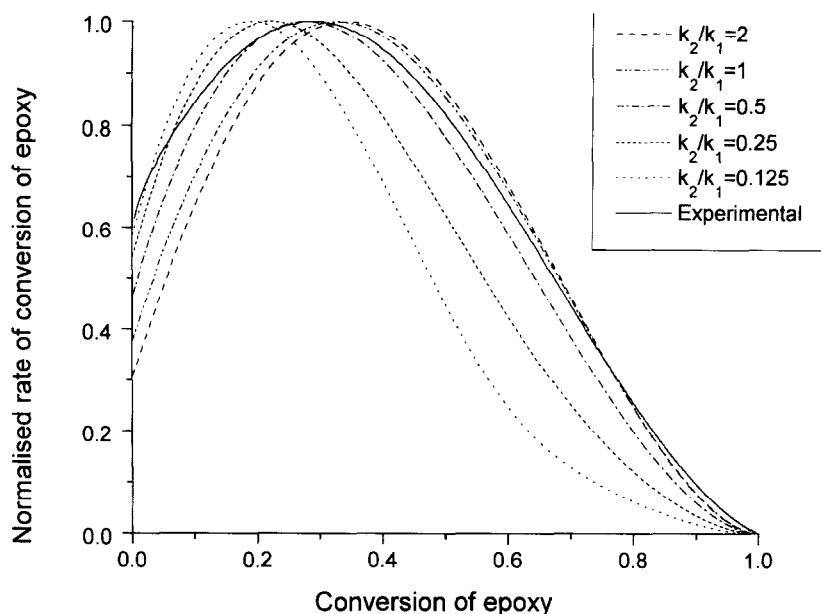


Figure 8 Normalized rate vs conversion showing the predicted effect of varying k_2/k_1 . The normalized data for DDM/DGEBA is shown for comparison

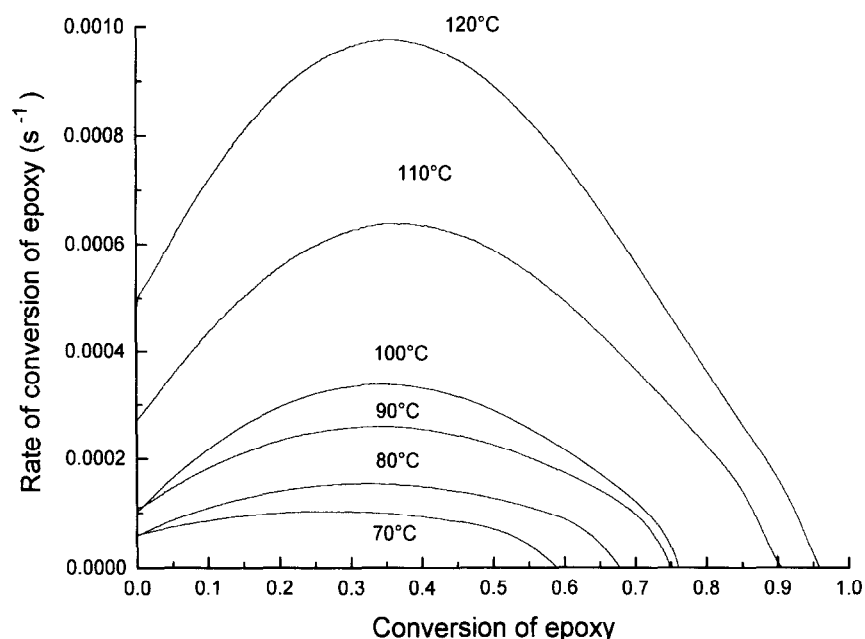


Figure 9 Experimental rate vs conversion for DGEBA/DDM from isothermal d.s.c. experiments at various temperatures

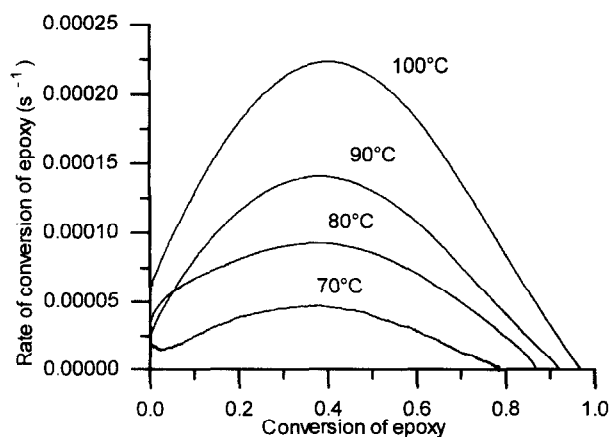


Figure 10 Experimental rate vs conversion for aniline/DGEBA from isothermal d.s.c. experiments at various temperatures

DDM/DGEBA system. As curing proceeds, the T_g of the aniline/DGEBA system rises due to increasing molecular weight and the concomitant loss of low molecular weight plasticizing components. In the systems containing DDM, the segmental mobility of the polymer should also be reduced by the formation of crosslinks²⁷⁻²⁹ so that the T_g for this system is dependent on the rise in molecular weight and loss of plasticizing species and, after gelation, on the degree of crosslinking that occurs during cure.

DiMarzio³⁰ derived a thermodynamic equation for the T_g of a network polymer based on the reduction in configurational entropy that occurs as crosslinking is increased. In this theory, the effect of crosslinking on the T_g of a polymer is given by:

$$\frac{T_g(X) - T_g(0)}{T_g(0)} = \frac{KX}{1 - KX} \quad (22)$$

where $T_g(X)$ is the T_g of a polymer with a degree of

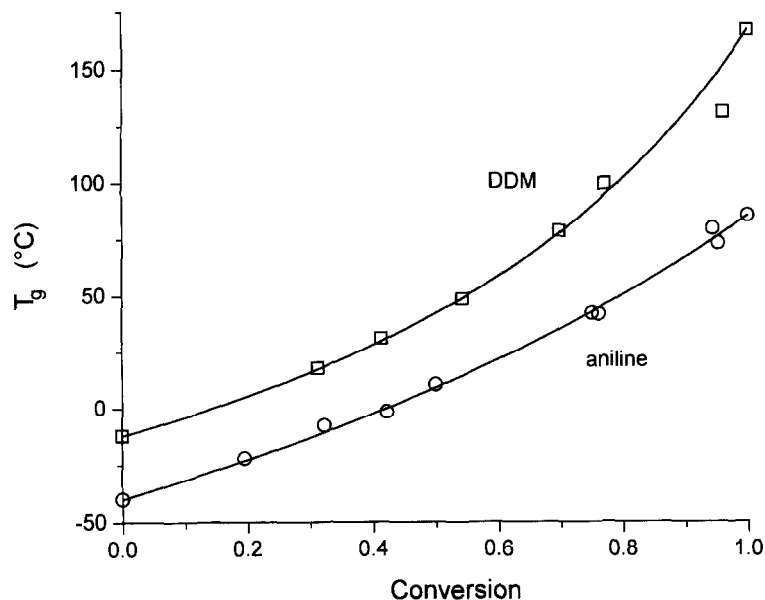


Figure 11 T_g vs conversion for DDM/DGEBA and aniline/DGEBA. The solid lines are theoretical fits to equation (25) using the values for $\Delta C_{p\infty}/\Delta C_{p0}$ of 0.57 for DDM/DGEBA and 0.80 for aniline/DGEBA

crosslinking X , $T_g(0)$ is the T_g of uncrosslinked linear polymer, and K is a dimensionless constant that is independent of the material to a first approximation²⁸. The difficulty with the application of this equation is that it does not include the effects of varying molecular weight, and the loss of plasticizing species that occurs in addition to crosslinking during cure³.

An alternative approach to this problem may be derived from the thermodynamic theory of Couchman and Karasz³¹, which describes the glass transition in copolymers by:

$$\sum x_i \int_{T_{gi}}^{T_g} \frac{\Delta C_{pi}}{T} dT = 0 \quad (23)$$

where ΔC_{pi} is the change in heat capacity of the component i at the glass transition temperature T_{gi} , and x_i is the amount of the component i in solution. Reasoning that a partially cured polymer is a solution of the polymer in the monomer and that the composition of the solution is related to the degree of conversion, Pascault and Williams³² adapted equation (23) to crosslinking systems by assuming that ΔC_p is proportional to $1/T$. Interestingly, Montserrat³³ has recently measured ΔC_p as a function of conversion and found a reciprocal relationship between ΔC_p and T_g , as assumed by Pascault and Williams³². The analysis by Pascault and Williams resulted in the following semi-empirical equation relating T_g to conversion:

$$T_g = \frac{(1 - \alpha)T_{g0} + \alpha(\Delta C_{p\infty}/\Delta C_{p0})T_{g\infty}}{(1 - \alpha) + (\Delta C_{p\infty}/\Delta C_{p0})\alpha} \quad (24)$$

where ΔC_{p0} is the heat capacity change at T_{g0} , the T_g of the monomer, and $\Delta C_{p\infty}$ is the heat capacity change at $T_{g\infty}$, the T_g of the fully cured network. Venditti and Gillham³⁴ used a similar approach with equation (23), but assumed that ΔC_p was constant, which resulted in a similar equation relating T_g and conversion:

$$\ln(T_g) = \frac{(1 - \alpha)\ln(T_{g0}) + (\Delta C_{p\infty}/\Delta C_{p0})\alpha \ln(T_{g\infty})}{(1 - \alpha) + (\Delta C_{p\infty}/\Delta C_{p0})\alpha} \quad (25)$$

Venditti and Gillham³⁴ have compared the applicability of equations (24) and (25) for a number of thermosetting systems using $\Delta C_{p\infty}/\Delta C_{p0}$ as a fitting parameter. In all cases the values of $\Delta C_{p\infty}/\Delta C_{p0}$ fitted with equation (25) were closer to the experimental values (obtained using d.s.c. measurements) than were those for equation (24).

Equation (25) was used to fit the experimental data by using the ratio of specific heat changes at the T_g of the fully cured material and uncured material $\Delta C_{p\infty}/\Delta C_{p0}$ as a fitting parameter. For the fits shown in Figure 11, the fitted parameters $\Delta C_{p\infty}/\Delta C_{p0}$ were calculated as 0.57 for the DDM/DGEBA system and 0.80 for the aniline/DGEBA system, which compare well with the experimental values of approximately 0.43 and 0.83 respectively. Fitting the same data to equation (24) (fits are not shown) with $\Delta C_{p\infty}/\Delta C_{p0}$ as a fitting parameter yielded values of 0.44 and 0.64 for DDM/DGEBA and aniline/DGEBA respectively.

According to the auto-catalytic rate model (see equation (21)), at zero conversion the kinetics depend only on the impurity catalysis reaction and the rate constant is given by K_{1c} . Thus we can obtain the activation energy and pre-exponential factor associated with this reaction, by measurement of the dependence of the rate constant at zero conversion (equal to K_{1c}) on temperature in the chemically controlled region. At 50% conversion both impurity catalysis and self-catalysis contribute to the kinetics. Thus the activation energy and pre-exponential factor for the autocatalytic reaction rate constant (equal to $K_1\alpha(1 - \alpha)^2$) can be calculated using the temperature dependence of the rate constant at 50% conversion and the previously calculated values of K_{1c} . Figure 12 shows Arrhenius plots taken from the isothermal d.s.c. data for the DDM/DGEBA system (Figure 9). The activation energies for K_1 and K_{1c} were 42 ± 5 and 52 ± 4 kJ mol⁻¹ for the autocatalytic and impurity reactions respectively, and the corresponding pre-exponential factors were $10^{3.4 \pm 0.6}$ s⁻¹ and $10^{3.6 \pm 0.5}$ s⁻¹.

Chemico-diffusion modelling to the epoxy-amine reaction was performed, at a particular temperature, by starting at zero conversion and iterating conversion by a

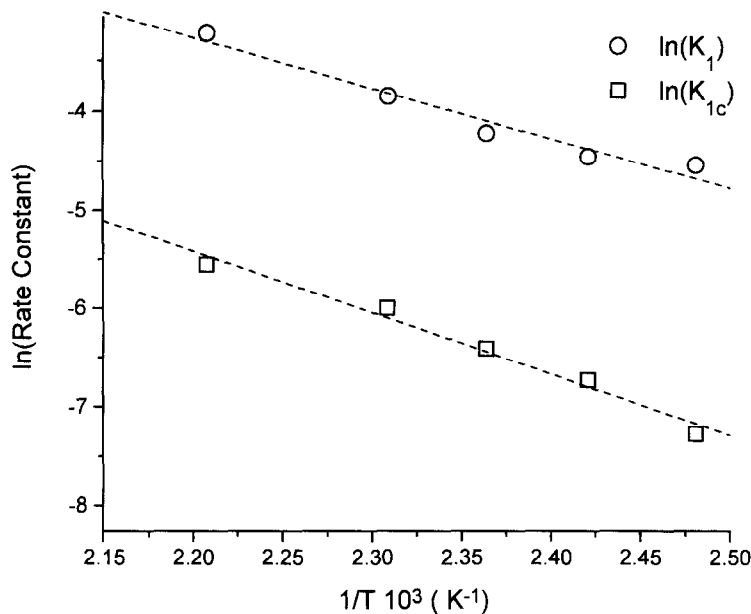


Figure 12 Arrhenius plot of rate constants for DDM/DGEBA using data extracted from Figure 9 at zero and 50% conversions

small amount. The chemical rate constants for both impurity and autocatalytic reactions were calculated for each level of conversion using equation (9). The T_g at the conversion under consideration was calculated using equation (25) and the diffusional rate constant was calculated from the combined WLF and Smoluchowski equations (see equation (15)). The commonly accepted values³⁵ of 40 and 52 K were used for the WLF constant C_1 and C_2 . The diffusion coefficients of small molecules in polymers at T_g are of the order³⁶ of $10^{-20} \text{ m}^2 \text{ s}^{-1}$. Using 0.5 nm as a typical value for the collision radius³⁷ yields an order of magnitude value for $k_{\text{diff}}(T_g)$ at T_g of 3.8×10^{-5} . The chemical rate constants ($K_1^{\text{(chem)}}$ and $K_{1c}^{\text{(chem)}}$) and diffusional rate constants ($K_1^{\text{(diff)}}$ and $K_{1c}^{\text{(diff)}}$) were combined using the Rabinowitch equation (equation (8)) to produce the overall rate constants (K_1 and K_{1c}) using the parameters in Table 1. These data were used to calculate the rate of conversion at a specific conversion using equation (21). The process of calculating rate constants and rate of conversion was

Table 1 Constants used in the chemico-diffusion model for DDM/DGEBA

Term	Equation where used	Value	From
$\Delta C_{p\infty}/\Delta C_{p0}$	Equation (25)	0.57	Figure 11
T_{g0}	Equation (25)	-10°C	Figure 11
$T_{g\infty}$	Equation (25)	165°C	Figure 11
$k_{\text{diff}}(T_g)$	Equation (15)	3.8×10^{-5}	Equation (13)
C_1	Equation (15)	40	WLF ³⁵
C_2	Equation (15)	52 K	WLF ³⁵
A_0 for K_1	Equation (9)	$10^{3.4} \text{ s}^{-1}$	Figure 12
ΔE for K_1	Equation (9)	41.5 kJ mol^{-1}	Figure 12
A_0 for K_{1c}	Equation (9)	$10^{3.6} \text{ s}^{-1}$	Figure 12
ΔE for K_{1c}	Equation (9)	51.8 kJ mol^{-1}	Figure 12

repeated for small increments of conversion until the reaction was complete or the overall rate dropped to a negligible level. Figure 13 shows the modelled rate vs conversion curves (calculated using the parameters listed in Table 1) corresponding to the experimental results for DDM/DGEBA in Figure 9. As can be seen, the modelled

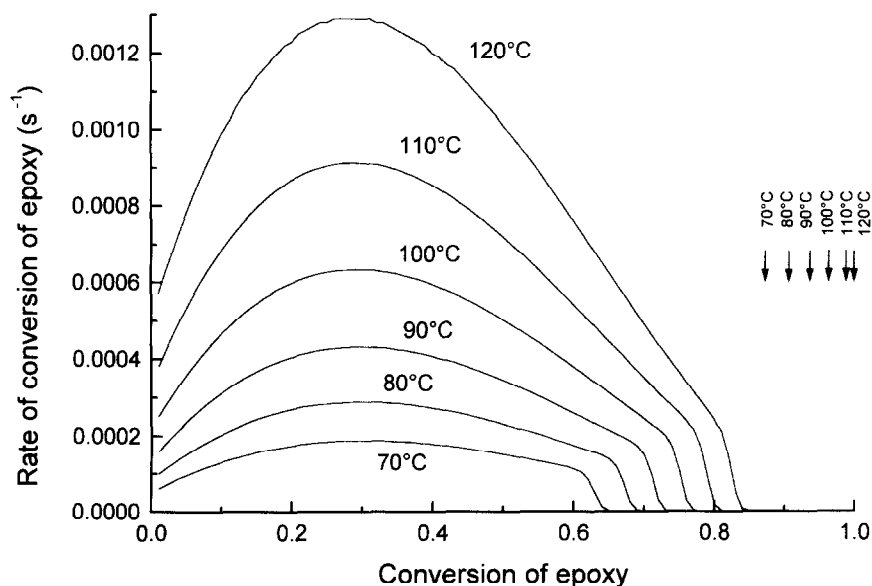


Figure 13 Modelled rate vs conversion for the DDM/DGEBA system using equations (8), (9), (15), (21), (25) and the parameters in Table 1. The arrows indicate the maximum conversion

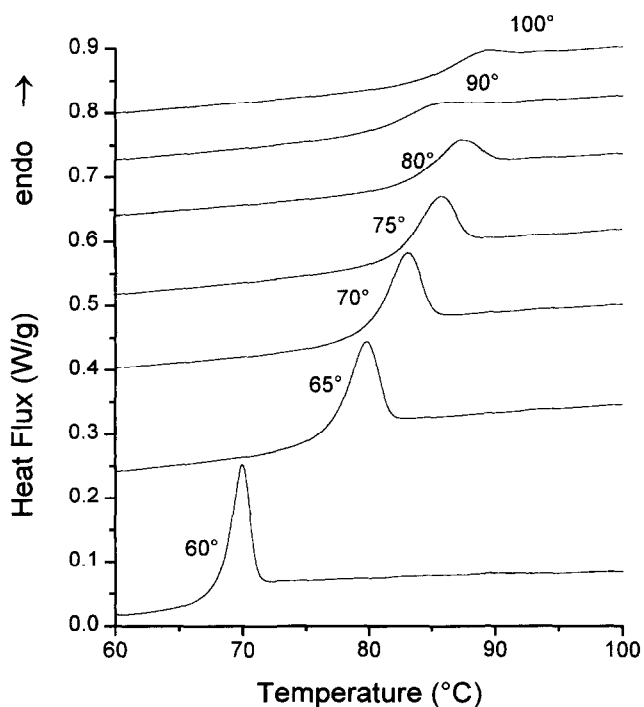


Figure 14 Scanning d.s.c. traces of aniline/DGEBA performed after isothermal cure at the temperatures indicated

curves have a similar form to the experimental results. The maximum rate occurs at approximately the correct conversion and the maximum conversion decreases as the temperature is lowered. However the predicted ultimate conversion do not correspond exactly with the experimental results, and the vitrification effect is more pronounced in the modelled data. The predicted curves show the rate passing through a maximum and then rapidly decreasing to a near zero value. Because the rate does not become zero until the T_g is somewhat above T_{cure} (as discussed later, at $T_{cure} + C_2$), the maximum conversion is higher than that readily apparent on the graph.

One possible reason for the lack of agreement between theory (Figure 13) and experiment (Figure 9) is that the

amine reaction cannot be characterized by a single pair of rate constants (k_1 and k_{1c}) because many different amine adducts are formed with a range of molecular weights and these may have different rates of diffusion (whereas a single rate constant was used in equation (15)) and thus different reaction rates in the diffusion controlled region. A distribution in rate constants would also tend to remove the sharp transition observed in the modelled curves at high conversions when the diffusional rate begins to control the reaction.

Another possibility for the discrepancy between the model (Figure 13) and experiment (Figure 9) is that the constants C_1 and C_2 used were not appropriate for the epoxy-amine system. An estimate of C_2 can be obtained from the dependence of T_g on cure temperature. Figure 14 shows the results of scanning d.s.c. experiments performed on aniline/DGEBA samples after maximum isothermal cure at various temperatures above and below the ultimate glass transition temperature ($T_{g\infty}$). A large ageing peak was present in d.s.c. scans after isothermal curing below $T_{g\infty}$ and this peak decreased in magnitude as the isothermal curing temperature was increased. Above the ultimate glass transition temperature for aniline/DGEBA (85°C), the ageing peak was very much smaller. The cause of this peak may have two contributions. Samples cured below $T_{g\infty}$ will vitrify during cure and thus undergo physical ageing, and polymers which are physically aged show an excess enthalpy overshoot in the scanning d.s.c. trace³⁸. In addition, as discussed below, isothermal curing below $T_{g\infty}$ results in incomplete cure, and these samples can recommence curing at higher temperatures thus causing an exotherm superimposed on the glass transition's sigmoidal step in heat capacity.

The data in Figure 14 and the data from similar experiments performed on the DDM/DGEBA system were used to produce the plots of T_g vs the curing temperature (T_{cure}) shown in Figure 15. It is well known that the curing temperature controls the T_g of the polymerization material^{3,4,12,23}. This occurs because as the T_g rises during cure, the diffusion rate slows until the reaction becomes diffusion controlled. Figure 15 shows

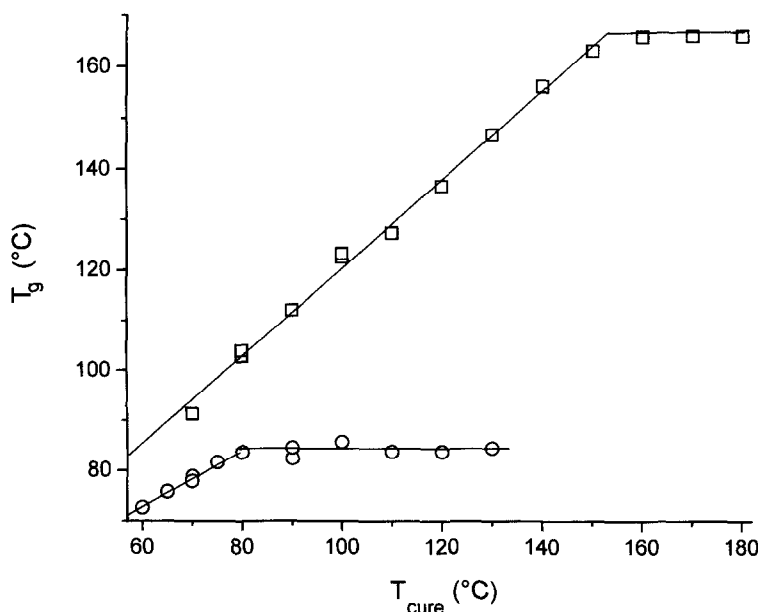


Figure 15 T_g vs T_{cure} for DDM/DGEBA (squares) and aniline/DGEBA (circles)

that in the DDM/DGEBA system at cure temperatures below the T_g of the fully cured material ($T_{g\infty}$), the measured T_g was 15–20°C above the curing temperature, while for the aniline/DGEBA system, the difference is close to 10°C. According to the WLF equation (equation (14)) diffusion should cease when $C_2 = T_g - T_{cure}$. Thus Figure 15 indicates that C_2 is between 15 and 20°C for DDM/DGEBA under the timescale of our experiments. However lowering C_2 and even varying C_1 failed to produce modelled curves that were significantly closer to the experimental results shown in Figure 9.

CONCLUSIONS

As part of a detailed study of the kinetic and thermodynamic factors involved in the toughening of networks by phase precipitation, the chemico-diffusion kinetics of network cure have been investigated using the model DDM/aniline/DGEBA epoxy-amine network forming systems. The DDM/DGEBA system was found to polymerize approximately twice as fast as the aniline/DGEBA system, due to an induction effect. For the high temperature cure data, the cure rate was analysed using the auto-catalytic model of Horie *et al.*⁴ and Smith⁵. Deviations between theory and experiment were discussed in terms of the substitutional effect for the amino-hydrogen groups and the etherification side reaction.

The extent of polymerization was dependent on the cure temperature, with low cure temperatures yielding lower rates of polymerization and lower degrees of cure. This was qualitatively interpreted in terms of the temperature dependence of diffusion and chemical reaction—at low temperatures, the rates of chemical reaction and of diffusion are lower, and as the material cures the glass transition approaches the curing temperature causing an abrupt reduction in diffusion rate and hence premature cessation of polymerization.

For quantitative analysis, the diffusion kinetics were modelled by combination of the WLF equation for the diffusion coefficient and the Smoluchowski equation¹³ for the diffusion rate, while the chemical rate constant for reaction was modelled by the Arrhenius equation. These two fundamental steps for a reaction—the diffusion of reactive groups into a state of encounter and the collisional reaction step—were combined using the Rabinowitch equation⁹. To determine the influence of degree of cure on T_g , d.s.c. scanning was performed up to a certain temperature and the T_g of the partially cured system subsequently measured. This T_g -conversion relation was well fitted to one of the Venditti and Gillham equations³⁴ derived from the Couchman-Karasz theory³¹. The experimental dependence of the reaction rate constant on conversion was reasonably well modelled by the theory. Deviations of experimental results from those predicted by theory were discussed in terms of the possible molecular weight dependence of the diffusion rate constant and the non-universal nature of the WLF constants. To investigate the latter possibility, isothermal curing studies were performed to determine the dependence of T_g on curing temperature. For curing conditions leading to incomplete cure, the T_g was approximately 15–20°C above T_{cure} for DDM/DGEBA and 10°C above for aniline/DGEBA, suggesting that for these systems the WLF constant, C_2 , is much less than the universal 50°C value. However, the application of values C_2 below the

universal value and variations in the value for C_1 did not significantly improve the modelled fit.

ACKNOWLEDGEMENTS

The authors would like to thank Dr John Charlesworth for helpful discussions on substitutional effects and Dr Ian Dagley for helpful comments, and to express thanks for the financial support of the CRC for Polymer Blends to CWW.

REFERENCES

1. Riew, C. K. and Gillham, J. K. (eds.), *Rubber Modified Thermoset Resins*, American Chemical Society, Washington DC, 1984.
2. Macosko, C. W. and Miller, D. R., *Macromolecules*, 1976, **9**, 198.
3. Wisanrakkit, G. and Gillham, J. K., *J. Appl. Poly. Sci.*, 1990, **41**, 2885.
4. Horie, K., Hiura, H., Sawada, M., Mita, I. and Kambe, H., *J. Polym. Sci., A-1*, 1970, **8**, 1357.
5. Smith, I. T., *Polymer*, 1961, **2**, 95.
6. Chern, C. S. and Poehlein, G. W., *Polym. Eng. Sci.*, 1987, **27**, 788.
7. Kim, D. S. and Kim, S. C., *Polym. Eng. Sci.*, 1994, **34**, 625.
8. Stutz, H., Mertes, J., Neubecker, K., *J. Polym. Sci., A: Polym. Chem.*, 1993, **31**, 1879.
9. Rabinowitch, E., *Trans. Faraday Soc.*, 1937, **33**, 1225.
10. Huguenin, F. C. A. E. and Klein, M. T., *Ind. Eng. Chem. Prod. Res.*, 1985, **24**, 166.
11. Deng, Y. and Martin, G. C., *Macromolecules*, 1994, **27**, 5147.
12. Havlicek, I. and Dusek, K., in *Crosslinked Epoxies*, ed. B. Sedlacek and J. Kahovec. Walter de Gruyter, Berlin, 1987, p. 417.
13. Smoluchowski, M., *Phys. Chem.*, 1918, **92**, 129.
14. Kummins, C. A. and Kwei, T. K., in *Diffusion in Polymers*, ed. J. Crank and G. S. Park. Academic Press, London, 1968, p. 120.
15. Durbetaki, A. J., *Anal. Chem.*, 1956, **28**, 2000.
16. Sue, C. C. and Woo, E. M., *Macromolecules*, 1995, **28**, 6779.
17. Mijovic, J. and Andjelic, S., *Polymer*, 1996, **37**, 1295.
18. Mijovic, J., Andjelic, S., Yee, C. F. W., Bellucci, F. and Nicolais, L., *Macromolecules*, 1995, **28**, 2805.
19. Barton, J. M., *J. Macromol. Sci.-Chem.*, 1974, **A8**, 25.
20. Rozenberg, B. A., *Adv. Poly. Sci.*, 1985, **75**, 113.
21. Ginsburg, D., *Concerning Amines*. Pergamon Press, Oxford, 1967, p. 65.
22. Charlesworth, J. M., *J. Polym. Sci., Polym. Chem. Edn*, 1987, **25**, 731.
23. Lunak, S. and Dusek, K., *J. Polym. Sci., Polym. Symp.*, 1975, **53**, 45.
24. Rozenberg, B. A., *Adv. Polym. Sci.*, 1985, **75**, 113.
25. Mijovic, J., Fishbain, A. and Wijaya, J., *Macromolecules*, 1992, **25**, 979.
26. Simon, S. L. and Gillham, J. K., *J. Appl. Polym. Sci.*, 1992, **46**, 1245.
27. Fox, T. G. and Loshaek, S., *J. Polym. Sci.*, 1995, **15**, 371.
28. Cook, W. D., *Eur. Polym. J.*, 1978, **14**, 715.
29. Charlesworth, J. M., *J. Macromol. Sci. Phys.*, 1987, **B26**, 105.
30. DiMarzio, E. A., *J. Res. Natl. Bur. Standards-A: Phys. Chem.*, 1964, **68A**, 611.
31. Couchman, P. R. and Karasz, F. E., *Macromolecules*, 1978, **11**, 117.
32. Pascault, J. P. and Williams, R. J. J., *J. Polym. Sci.: Polym. Phys.*, 1990, **28**, 85.
33. Montserrat, S., *Polymer*, 1995, **36**, 435.
34. Venditti, R. A. and Gillham, J. K., *Polym. Mater. Sci. Eng.*, 1993, **69**, 434.
35. Ferry, J. D., *Viscoelastic Properties of Polymers*. Wiley, NY, 1970, p. 317.
36. Kim, H., Waldow, D. S., Han, C. C., Tran-Cong, Q. and Yamamoto, M., *Polym. Commun.*, 1991, **32**, 108.
37. Adamson, A. W., *A Textbook of Physical Chemistry*, 2nd edn. Academic Press, NY, 1979, p. 612.
38. Montserrat, S., *J. Appl. Polym. Sci.*, 1992, **44**, 545.